IDŐJÁRÁS

Quarterly Journal of the Hungarian Meteorological Service
Vol. 115, No. 3, July–September 2011, pp. 179–204

Air quality around motorway tunnels in complex terrain – computational fluid dynamics modeling and comparison to wind tunnel data

Márton Balczó[1*], Miklós Balogh[1], István Goricsán[1], Torsten Nagel[2], Jenő M. Suda[1], and **Tamás Lajos[1]**

[1]*Theodore von Kármán Wind Tunnel Laboratory, Department of Fluid Mechanics, Budapest University of Technology and Economics (BME), Bertalan L. u. 4-6, H-1111 Budapest, Hungary*
E-mails: balczo@ara.bme.hu; baloghm@ara.bme.hu; goricsan@ara.bme.hu; suda@ara.bme.hu; lajos@ara.bme.hu

[2]*Lohmeyer Consulting Engineers*
An der Roßweid 3,76229, Karlsruhe, Germany
E-mail: t.nagel@lohmeyer.de

[*]*Corresponding author*

(Manuscript received in final form September 21, 2010)

Abstract—The current paper describes numerical simulations of flow and dispersion performed in a complex suburban area of Budapest using the microscale model MISKAM and accompanying wind tunnel tests which provided reference concentration data for validation of the model results. Main pollutant sources are traffic related and include a planned motorway section of 9 km length consisting of sections running in tunnel, on ground, and on viaduct. Four different route alternatives were investigated. In the paper, first a condensed review is given about problems related to air quality around motorway tunnels in complex terrain. The effect of larger scales on microscale air quality was determined using background concentrations from monitoring station time series with removal of short-term fluctuations, for which a simple method is introduced here. The validation wind tunnel tests were carried out at several wind directions on a 1:1000 scale model containing topography, buildings, and vegetation with measurement of tracer concentrations in 50 sampling locations. In the microscale CFD simulation, flow and dispersion considering topography, vegetation, and buildings were calculated three-dimensional in a large domain using k–ε model, and advective diffusion equation was set up on a Cartesian grid treating air pollutants as non-reactive scalars. Results give more detailed information about the flow, for example local speedup above hills, slowdown in vegetation zones, separation regions are resolved well. Deviation of pollutant plume paths from the mean wind direction caused by the topography could be also observed. NO_x concentration maps showed that air quality limit exceedances occur near motorway tunnel portals in form of large surface plumes, which can only be avoided by the application of

tunnel ventilation stacks. These will exhaust polluted tunnel air in larger heights. The comparison of numerical results to the wind tunnel reference data was performed using statistic metrics (fractional bias, normal mean square error, geometric mean bias, geometric variance, correlation coefficient) showing a generally good agreement.

Key-words: air quality, complex terrain, tunnel portal, CFD simulation, background concentration, model validation, wind tunnel measurement

1. Introduction

The prediction of air quality in urban or suburban areas often requires sophisticated tools when the surrounding terrain is complex. The major pollutant sources are mostly traffic related, emitting pollutants along main road or motorway routes. Buildings and vegetation have also strong influence on the dispersion process. Additional problems can emerge due to the concentrated exhaust of polluted air from roadway tunnel portals. A short literature overview of these topics will be given in the following subsections, followed by a short description of the investigated area in the north of Budapest, which includes, besides existing main roads, a 9 km long planned motorway section with longer tunnels. Section 2 discusses the proper input data collected for the microscale numerical simulations and wind tunnel tests, which are then described in detail in Section 3. In Section 4, we give an overview of the CFD results and compare them to the wind tunnel data. Additionally, we also summarize the proposed arrangements for reducing air pollution from the tunnel portals.

1.1. Flow over complex terrain

Complex terrain can produce a variety of flow patterns, mainly depending on the topography, vegetation cover, and the thermal stratification (Froude number), as described in standard texts, for example in *Plate* (1982) and *Kaimal* and *Finnigan* (1994). Basic mechanisms are discussed by *Belcher* and *Hunt* (1998), and an overview of research in the last 50 years is given by *Wood* (2000).

To validate the modeling tools for complex terrain flows, numerous studies were performed. Beyond isolated and simplified 2D or 3D slopes and hills measured in wind tunnels (e.g., *Ayotte* and *Hughes*, 2004), the Askervein hill project (*Taylor* and *Teunissen*, 1987; *Walmsley* and *Taylor*, 1996) has gained specific importance, with an on-site measurement campaign being performed in 1982–1983, which served as reference data for dozens of wind tunnel and numerical studies. The wind tunnel method gave good agreement with the measurement reference data (see e.g., particle image velocimetry (PIV) measurements of *Rodrigues*, 2005). *Bowen* (2003) discusses aspects of physical modeling like model scale and roughness in detail. In CFD modeling, besides the Reynolds-averaged Navier-Stokes (RANS) approach using mostly k–ε turbulence closure (*Kim* and *Patel*, 2000; *Castro et al*., 2003), in the last decade

even more large-eddy simulation (LES) was used to model the Askervein hill flow (e.g., *Silva Lopes et al*., 2007).

The application focus of the practical studies in this field is on wind turbine siting, heavy gas dispersion, and the determination of airport wind conditions. Several authors reported wind tunnel tests of real-world, very complex terrain. *Cermak* (1984) performed tests for different stratifications. Further studies to mention are those of *Snyder* (1990), *Liu et al.* (2001), and *McBride et al.* (2001). Numerical application examples using a RANS k–ε model and comparison with on-site measurements are shown for example in *Brodeur* and *Masson* (2006) and *Palma et al.* (2008).

1.2. Tunnel related air quality problems

In roadway tunnels, a large amount of traffic pollution can be accumulated, which is removed by the pressure difference, the piston effect of moving vehicles, and the tunnel ventilation system mostly through the tunnel portal. The tunnel ventilation system for one directional tunnel of medium length consists of axial fans mounted in the tunnel pipe, which drive air into the driving direction and exhaust polluted air at the forward tunnel exit. An overview of tunnel related air quality problems is given by *Longley* and *Kelly* (2008) and *Bettelini et al.* (2001), the latter is also showing modeling results near a tunnel portal with a Gaussian model and CFD. *Oettl et al.* (2003) compared results from two specific portal dispersion models with on-site measurements.

Wind tunnel measurements of a tunnel portal with moving vehicles were reported by *Nadel et al.* (1994) and *Plate* (1999). They observed high concentrations near the portal and recognized the influence of traffic induced turbulence. *Contini et al.* (2003) measured flow and dispersion near tunnel portals behind a 2D hill. Tunnel emissions were released from a point source in the middle of the tunnel.

Tunnel ventilation systems are designed according to national standards like those of Switzerland (*ASTRA*, 2004). To avoid large concentrations outside the portals of longer tunnels, it is often necessary to install separate ventilation stacks which direct polluted air from the tunnel into larger heights or filter facilities which remove a part of pollutants.

1.3. Site description

The area of investigation covers about 8 km × 5 km. The topography has moderate slopes similar to Askervein hill, with height differences of about 200–300 m (*Fig. 1*). In the south-eastern part of the domain, outskirts of Budapest are located with 10–15 storey block buildings and a population of about 70,000. On the northern and western side, four suburban towns can be found in the complex terrain of Buda Mountains with 20,000 inhabitants. Deciduous forests cover a smaller part of the not habited areas, mainly hilltops.

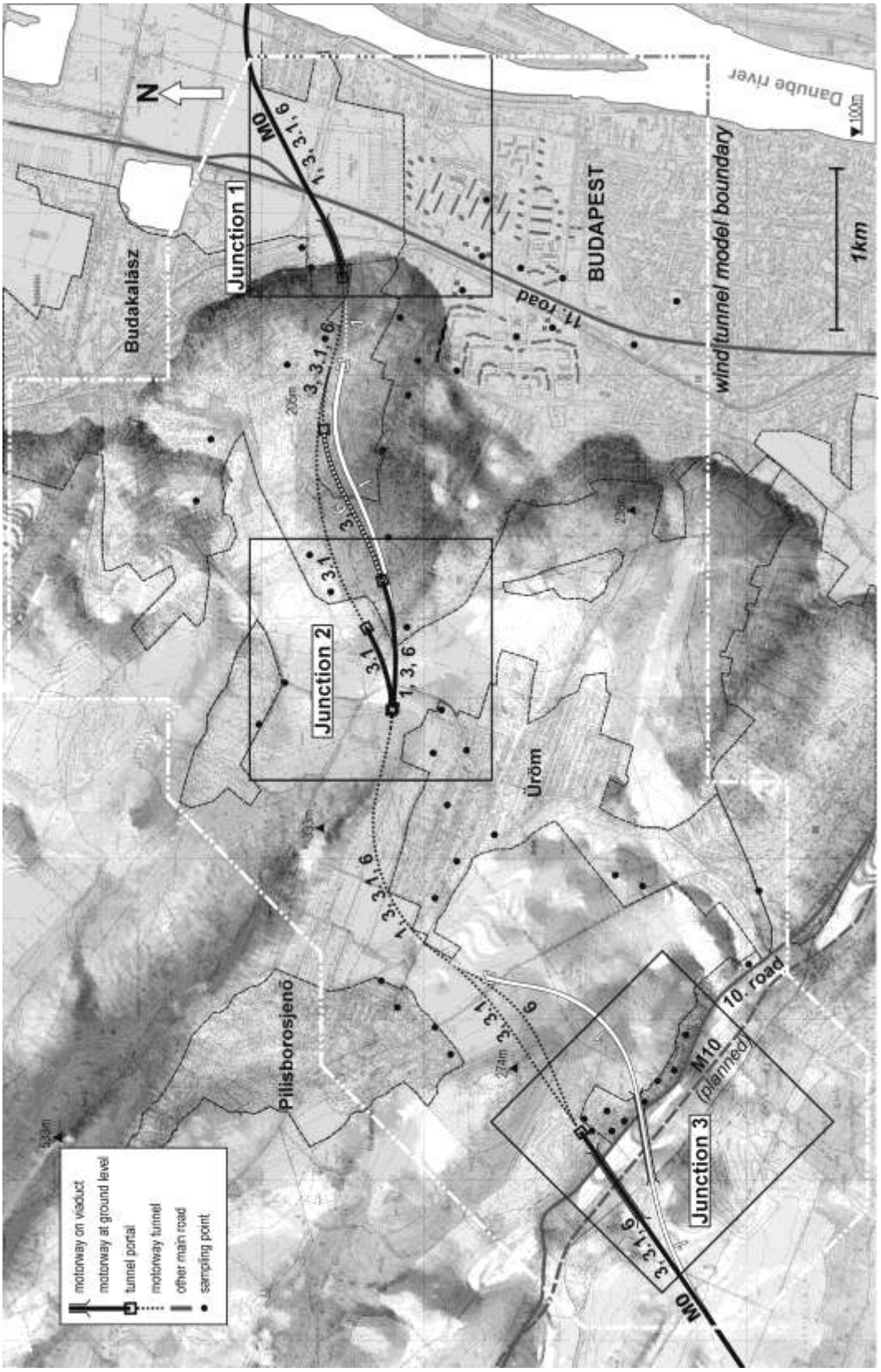

Fig. 1. The investigated domain with existing main roads and planned route alternatives 1, 3, 3.1, and 6 of the M0 motorway. Route colors are black or white. Please note that the routes are partly overlapping. Circular black dots: wind tunnel sampling points (50); thin continuous black rectangles: close investigation areas of numerical simulation in the 3 junctions; thin dashed line: inhabited areas.

Major pollutant sources are traffic sources, existing main roads (national roads No. 10 and No. 11) and most importantly, a planned section of the ring motorway M0 of Budapest, consisting of three traffic junctions. Four route alternatives have been investigated: 1, 3, 3.1, and 6, all of them include several bridges and tunnels.

The planned ring motorway section connects national road No. 10 and planned motorway M10 in the northwest of Budapest with national road No. 11 in the north of Budapest. Route 1 (marked white in *Fig. 1*) is the most southern from the alternatives, and has shorter tunnels. Route 3.1 and 6 differ from route 3 only in the middle and eastern part: route 6 runs in Junction 2 longer eastwards on surface and has a shorter eastern tunnel. Route 3.1's surface section and eastern tunnel's portal in Junction 2 are shifted to the north. On the far eastern side, in Junction 1 near the national road No. 11, all routes are identical. In Junction 1 and 3, the routes cross the valleys on viaducts. In Junction 2, the routes run in deep cutting.

Rush-hour traffic on the new section is expected to reach about 2,800 vehicle h^{-1} in the year 2018 with further growth to 4,400 vehicle h^{-1} until 2023. The planned one-directional tunnels are up to 3.2 km long, and their original design included longitudinal ventilation using axial fans without separate ventilation stacks (see later in *Fig. 10*). As a consequence, all pollutants produced in the tunnel are supposed to leave the tunnel through the forward portal.

Due to the closeness to inhabited areas, air quality and noise impacts of the new motorway were of most concern. The availability of high-resolution pollutant concentration maps of the area is thus crucial for the decision makers to help them find the best route alternative, and also for the public[1] to accept the selected route.

2. Input data

Unlike the investigations, focusing on the dispersion phenomenon itself, at the end of environmental impact assessment studies like this, exact concentrations should be calculated as a decision basis for the authorities. Any errors in input data like background concentrations, wind statistics, or car emissions will also be reflected in the results. Thus, one has to pay specific attention to the collection of high-quality input data.

2.1. Background concentrations

Pollutant dispersion is a multi-scale process in both space and time. Besides the possibility of a full coupling of different scale models (nesting), a demanding task for modelers, the usual approach is to consider the effect of larger scales in the microscale dispersion model as a background concentration. The background

[1] Short reports prepared for the public about this project can be found at www.karman-wtl.com (in Hungarian).

concentration might be significantly different in urban and rural areas, and can be determined in several ways: (a) by taking the output of a mesoscale / urban scale model or (b) using measurement data from urban background stations.

In *Mensink et al.* (2008), coupling of the Gaussian mesoscale dispersion model IFDM and the street canyon scale model OSPM was realized. Example of the second method can be seen in *Berkowicz* (2000), a simple urban background model developed for Copenhagen, using the urban emission inventory, rural background measurement data, and wind statistics.

When applying the second method, one has to consider the fact that urban background stations are also subject to short-term variations due to local pollution sources. Their effect should hence be removed to obtain clean background values. *Cremades* (2000) demonstrated two methods for this in a hypothetical case, while *Jones et al.* (2008) removed the effect of nearby traffic sources by comparing weekend and weekday concentrations at an urban monitoring station in London and determined the urban background values and urban non-traffic increments of PM_{10} . *Tchepel* and *Borrego* (2010) analyzed spectra of air quality monitoring data using spectral methods and found that short-term fluctuations correlate with daily variations in traffic and wind speed. Long-term variance over a 21-day period caused by long-range pollutant transport was also observed. In *Tchepel et al.* (2010), after spectral analysis of the concentration time series, short-term components above a frequency threshold were flattened using the Kolmogorov-Zurbenko filter.

In the present case, data from two background stations in Budapest were analyzed for the years 2007–2008. Pesthidegkút station is located in a suburban area, and thus, it is characteristic for Junction 2 and 3, while Gilice tér station is in an outer district of the city, which can provide background data for the semi-urban environment of Junction 1 (*Fig. 1*). Both stations are influenced by local sources with daily peaks in the morning and afternoon rush-hours (*Fig. 2*), especially for NO_x, which indicates a relatively close traffic release.

This local influence was removed by separating the baseline and short-term parts of the time series using Fourier transformation.

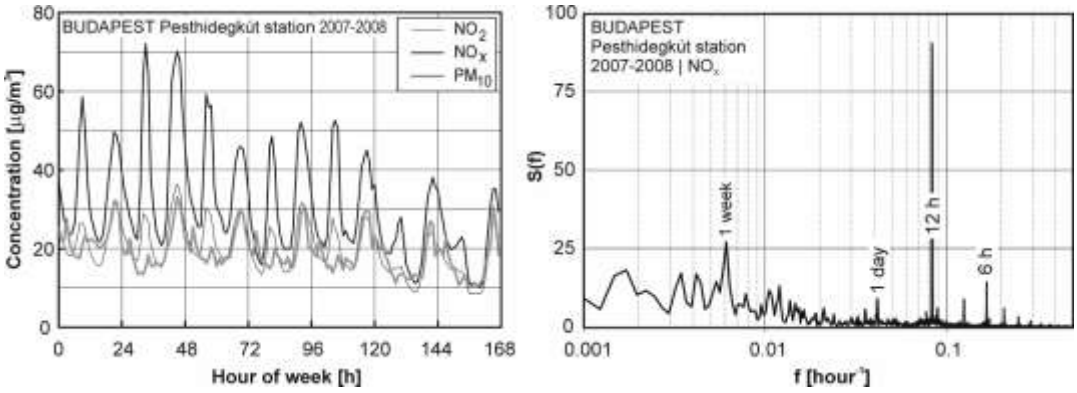

Fig. 2. Left: Average weekly concentrations at Pesthidegkút station in Budapest; right: spectrum of NO_x concentrations with a strong 12 h peak.

Because local traffic influence is reflected in the strong 12 h and 6 h components of the FFT spectrum (*Fig. 2*), the separation frequency was chosen as $0.056\ h^{-1}$, corresponding to the period of 18 h. After the separation, the average absolute value of the short-term signal was subtracted from the mean value of the original time series to obtain the annual mean background concentration without the contribution of local sources (*Table 1*).

Table 1. Background concentrations [$\mu g\ m^{-3}$]

	Annual mean		**Fluctuations removed**	
	NO_x	**PM_{10}**	**NO_x**	**PM_{10}**
Budapest, Pesthidegkút[a]	31.5	19.2	15.8	13.2
Budapest, Gilice tér[b]	39.6	31.2	20.0	20.4

[a] Suburban background station, 47.5617°N, 18.9608°E, Junction 2 and 3

[b] Urban background station, 47.4298°N, 19.1812°E, Junction 1

2.2. Emissions

Car emissions can be determined from traffic density and the emission factors of different vehicle categories. These are again dependent from fleet composition, traffic situation, slope, and so on. In this project, fleet-average emission factors for the reference year 2006 and realization year 2018 had to be determined. The Handbook of Emission Factors – HBEFA 2.1 (*Infras*, 2004) is the emission factor database of several mid-European countries (D, A, CH, NL) based on emission factors determined for individual vehicle groups, the so-called vehicle subsegments. Vehicles of the same class, engine power, and emission category have obviously similar emission factors, which were determined by dynamometer measurements. These may vary depending on traffic situation, speed, slope, road quality, and temperature. The accumulated emission factor valid on a specific road section (urban, rural, motorway etc.) is then an average of subsegment factors weighted by the actual traffic composition, which is also included in the database. The method was validated in several studies, e.g., through emission measurements in the Gubrist tunnel by *Colberg et al.* (2005).

To apply the method in Hungary, the national vehicle database of the years 2001–2006 was analyzed, and the fleet was divided into vehicle subsegments defined in the HBEFA database. As a rough estimate, a four-year delay compared to the vehicle fleet in Germany was demonstrated for passenger cars and light duty vehicles[2].

[2] In the meantime, the new HBEFA version 3.1 was released, supporting also vehicle fleets of Norway and Sweden. Further validation of emission factors and the new emission models applied lead in the upgrade to higher NO_x and PM emission factors for passenger cars and lower ones for light and heavy-duty vehicles. These changes might increase the accuracy of the concentration predictions, however, it could not anymore considered in this paper.

The fleet-averaged emission factors for the M0 motorway with 80 km/h speed limit and ±2% slope are shown in *Table 2*. The general improvement of factors over the years is due to the replacement of older vehicles with vehicles that comply with the EURO4 and newer standards. Also, non-exhaust PM_{10} emissions from abrasion and resuspension were considered, based on an on-site measurement campaign along a motorway (*Ketzel et al*., 2007).

Table 2. Accumulated exhaust and non-exhaust emission factors [g km^{-1} veh^{-1}] for different vehicle categories calculated from the subsegment emission factors of the HBEFA 2.1 database and Hungarian fleet composition data. Traffic situation: motorway with 80 km/h speed limit and ±2 % slope

Emission factor	**NO_x**		**PM_{10}[a]**		**$PM_{10,\ n\text{-}e}$[b]**
Year	**2006**	**2018**	**2006**	**2018**	**All years**
Passenger car	0.60	0.17	0.008	0.007	0.022
Light duty vehicle	1.17	0.54	0.193	0.034	0.022
Coach	7.86	3.66	0.494	0.052	0.200
Heavy duty vehicle	5.04	2.81	0.120	0.037	0.200

[a] exhaust factors

[b] non-exhaust factors (*Ketzel et al.*, 2007)

2.3. Wind statistics

Long-term wind statistics were only available at a station of the Hungarian Meteorological Service (HMS) about 5 km from the site in a flat area. To determine local wind statistics, which may be different from the flat terrain measurements and could show systematic mesoscale changes due to the Buda Mountains, the mesoscale diagnostic wind field model DIWIMO[3] was run on a 30 km × 16.3 km domain shown in *Fig. 3*. Elevation in this domain varies between 87 and 562 m above sea level.

The model generates a mass-consistent wind field based on the measured wind statistics in one point of the domain considering the topography, stratification, varying surface roughness, and surface coverage of the area. The model's parameterizations are described in detail by *Moussiopoulos et al.* (1988).

The model uses a terrain-following mesh, in the current simulation with a horizontal grid resolution of 100 m, while in vertical direction the domain of 800 m height was divided into 26 layers of varying thickness. The lowermost layer's thickness changed between 7 and 19 m due to the stretching of the vertical grid to the terrain.

[3] Further description can be found at www.stadtklima.de/EN/E_1tools.htm#DIWIMO and on the webpage of Lohmeyer Consulting Engineers: www.lohmeyer.de/modelle/diwimo.htm (in German).

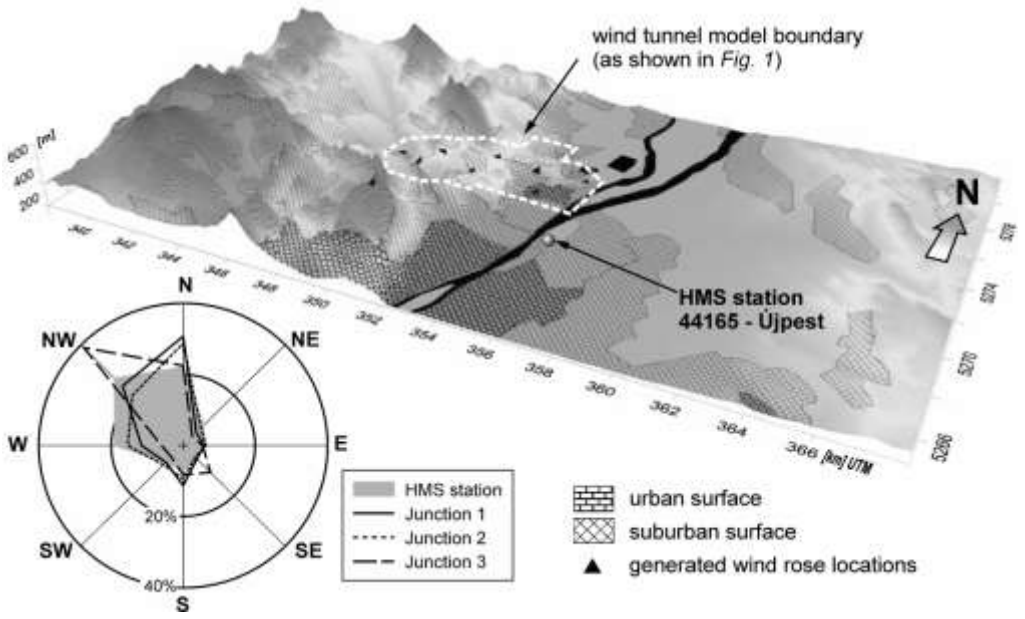

Fig. 3. Top: Domain of DIWIMO simulation with land usage patterns and generated wind rose locations. Elevation is scaled by 5. Bottom left: original wind statistics of the HMS station simplified for eight main wind directions (grey plot); mean wind roses, averaged from all calculated wind roses in the specific junction.

The model was run with 36 wind directions, and wind statistics were generated at 9 locations in the closer investigation area (3 in each traffic junction) using the known wind statistics at the location of the HMS station. These were averaged in each of the three junctions and simplified for the 8 main wind directions. The averaged wind roses can be seen as representative for the individual junctions, and can also be used as inlet boundary condition for the microscale investigation of the junctions.

In Junction 1 and 2, the wind roses show higher mean wind speed and distortions due to topographic effects towards the north (*Fig. 3*, bottom left). At Junction 3, influence of a NW–SE oriented valley can be clearly recognized. Based on the wind statistics, 5–7 important incident wind directions were selected at each junction for further microscale investigation, covering about 80% of the wind conditions in a year.

3. Microscale investigation methods

3.1. MISKAM flow and dispersion simulations

In the last decade, dozens of different CFD models were developed and applied for the investigation of microscale air pollution problems, where the effect of a singular or a group of obstacles is not negligible, and thus, the solution of the full equations of motion is necessary. On behalf of the numerous publications in this topic, most of them are concentrating on built urban areas, more specifically

street canyons, only the reviews of *Vardoulakis et al*. (2003) and *Holmes* and *Morawska* (2006) may be cited here. Besides the models utilizing the RANS (Reynolds-averaged Navier-Stokes) approach with k–ε type turbulence closures, large-eddy simulation is applied with promising results (e.g., *Xie* and *Castro*, 2009), however, on the price of a very high computational demand (needing multi-processor computer clusters), which is in most cases not accessible for environmental agencies and consulting engineers.

The code used in the current investigation, MISKAM gained currency in environmental assessment practice due to the relatively simple model setup and the fast code able to run on a single processor PC. The model solves the RANS equation using a k–ε turbulence closure on a Cartesian grid. Buildings are represented as blockouts from the grid. Dispersion of an inert pollutant is calculated afterwards by the advection-diffusion equation using the wind field simulation results. Vegetation effects can be accounted for by additional terms in the flow and turbulence equations. Details of the MISKAM model are given in *Table 3* or in more depth in *Eichhorn* (2008).

Extensive model evaluation activities were undertaken according to *VDI* (2005) by *Eichhorn* and *Kniffka* (2010) and in the framework of COST Action 732[4] (*Goricsán et al*., 2011) using the MUST data set. The implemented vegetation model (*Ries* and *Eichhorn*, 2001), which introduced additional terms in the motion and turbulence equations, was validated in *Balczó et al.* (2009) using the CODASC[5] wind tunnel data set.

Besides these, the model has been used in several validation and comparison studies. *Ketzel et al.* (2000) compared MISKAM data to on-site measurements, as it was also done in the Podbi-exercise (*Lohmeyer et al*., 2002). Comparison of MISKAM simulation data to urban wind tunnel measurements can be found in *Ketzel et al*. (2002), *Sahm et al*. (2002), *Goricsán et al.* (2004), and for a simple stack-building configuration in *Olesen et al.* (2009). Several authors used MISKAM results as input for other transport and chemistry models (*Stern* and *Yamartino*, 2001; *Dixon* and *Tomlin*, 2007), or for emergency response tools (*Donnelly et al*., 2009).

Although MISKAM is able to model the effect of stable stratification on dispersion by decreasing turbulence production in the equations of k and ε, and in general, CFD modeling of stratification and thermal induced flows is possible (see, e.g., the adaptation of CFD solvers for stratified flows in *Kristóf et al*., 2009), in this case we limited the influence of thermal stratification to neutral conditions to preserve the compatibility of CFD results with the wind tunnel measurements.

---

[4] COST Action 732: Quality Assurance and Improvement of Micro-Scale Meteorological Models, www.mi.uni-hamburg.de/Home.484.0.html

[5] CODASC data base, (COncentration DAta for Street Canyons), Laboratory of Building and Environmental Aerodynamics, IfH Karlsruhe Institute of Technology, www.codasc.de

Table 3. Description of the MISKAM model

Model equations	
Model version	MISKAM 5.01
Flow model	Reynolds-averaged Navier-Stokes equation with turbulence closure
Turbulence model	Modified version of Kato-Launder k–ε (*Kato* and *Launder*, 1993*; López*, 2002)
Model constants	$C_\mu = 0.09$, $C_{\varepsilon 1} = 1.44$, $\sigma_\kappa = 1$, $\sigma_\varepsilon = 1.3$, $\kappa_\mu = 0.4$
Wall treatment	Logarithmic wall function
Vegetation treatment	Porosity-based model
Dispersion model	Reynolds-averaged advective diffusion equation
Turbulent Schmidt number	0.74
Numerical schemes	
Order in time	1st order explicit
Advection terms	
– momentum equation	Upstream
– dispersion equation	MPDATA scheme (*Smolarkiewicz* and *Grabowski*, 1989)
Diffusive terms	ADI (Alternating Direction Implicit) method
Computational grid	
Grid type	Arakawa-C non-equidistant Cartesian grid (staggered grid), with buildings and topography blocked out from the grid
Variable definition	u, v, w defined at the centre of the corresponding face of the cell, scalar quantities defined at the centre of the cell
Boundary conditions	
Flow variables	
Inlet velocity profile	Logarithmic profile with roughness length z_0 fitted to reference height H_{ref} and velocity u_{ref}
Inlet turbulence profile	Generated from the assumption of equilibrium boundary layer
Ground \& building surfaces	No-slip (with wall function)
Top boundary	Constant values of u, v, w, k, ε taken from the top of the inlet profile
Lateral boundaries	No-flux
Outflow boundary	No-flux with pressure correction to ensure overall mass conservation
Dispersion variables	
Inflow boundary	$c = 0$
Lateral and outflow boundaries	No-flux
Source cells	Volume source strength Q with optional vertical momentum w prescribed
Vegetation cells	Leaf drag coefficient $c_D = 0.2$ and *LAD* (leaf area density) prescribed

The computational domains and grids were created following the Best Practice Guideline of *Franke et al.* (2007) using an in-house preprocessor. In each junction, close investigation areas of 1.5 km × 1.5 km were defined (see black rectangles in *Fig. 1*), for which grids of uniform horizontal resolution were generated. Inflow and outflow zones of sufficient length were attached to these to prepare correct inflow conditions in the investigated area (*Fig. 4*).

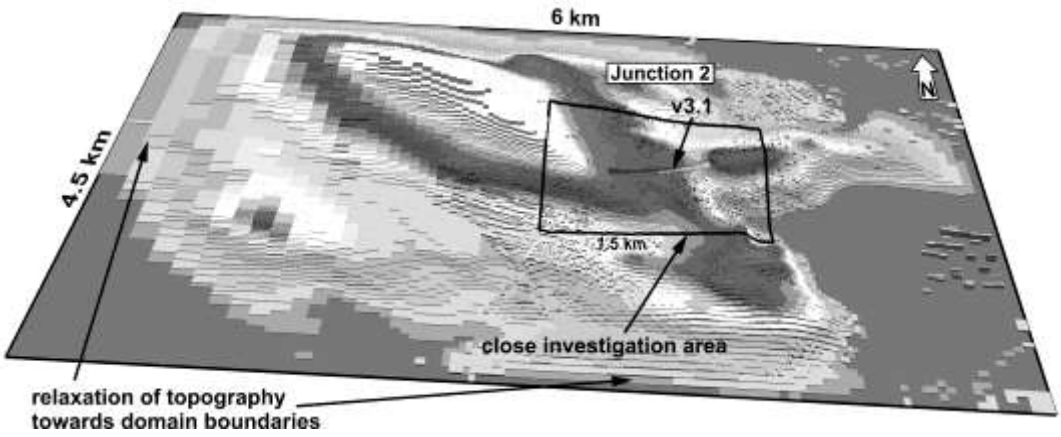

Fig. 4. View of the MISKAM model domain of Junction 2 showing the non-uniform grid with the highest grid resolution around the two tunnel portals and the relaxation of topography at the boundaries.

The domain height was 2 km to ensure a low blockage ratio of 3%. Terrain height sunk to zero at the boundaries. The cell number of each grid was above 5 million. The simulation time on a 3 GHz Intel Core2 computer was about one week for a case. Further details of the simulations are given in *Table 4*.

Table 4. Grid and simulation details. In each junction, simulations were run for every wind direction and every source, resulting in a high number of simulations

	Unit	**Junction 1**	**Junction 2**	**Junction 3**
No. of grid cells	–	246 × 255	206 × 321	252 × 273
– vertical direction	–	97	77	97
Highest resolution	m	5 × 7.5		
– vertical direction	m	1.5		
Max. cell growth ratio	–	1.2		
Cell number	million	5.526	5.244	5.225
Wind directions investigated	–	N, SE, S, WSW, W, WNW, NW	N, NE, S, W, NW	N, SE, S, W, NW
Leaf area density	$m^2\ m^{-3}$	0.5 (in forest areas)		
Vent. stack vertical velocity	$m\ s^{-1}$	6		
No. of dispersion simulations	–	107	92	52

3.2. Source treatment and simulations on a simplified tunnel model

Traffic pollutants released in a one-directional motorway tunnel are exhausted usually through the forward tunnel portal in a low-speed jet. In the MISKAM simulations, as it is not allowed for the user to prescribe horizontal momentum, this jet was replaced by a point source without momentum located in a certain

distance in front of the tunnel portal. To justify the above simplification, several numerical simulations were performed using the more flexible FLUENT code. The FLUENT 6.3 simulations used a simple tunnel portal geometry shown in *Fig. 5* on the left.

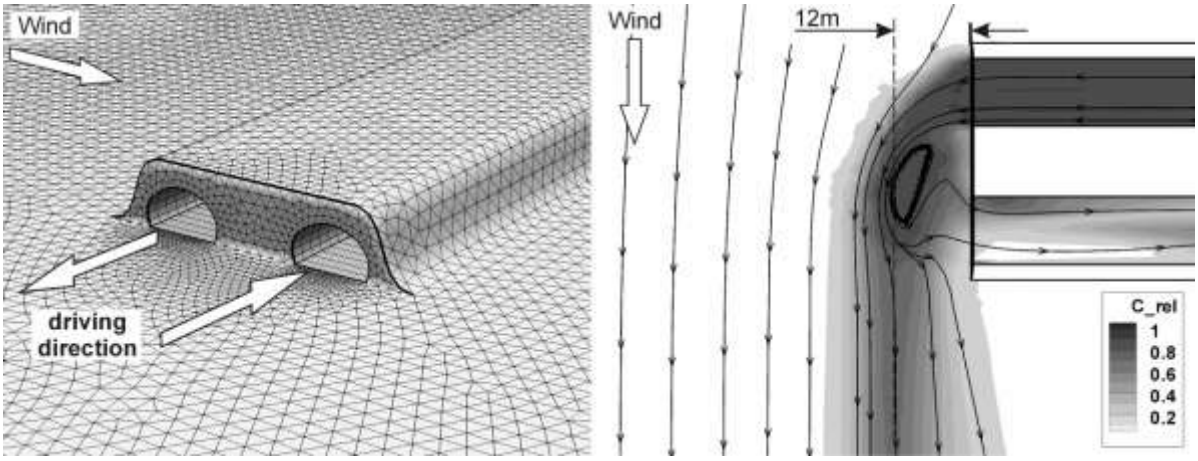

Fig. 5. Left: simplified tunnel geometry and grid for the preliminary investigation of flow around the portals using FLUENT with tunnel cross-section of 12 m × 6.5 m, portal height 10 m, tunnel axis distance 24 m. Right: simulation results in a horizontal cross-section at 3 m height with streamtraces and relative concentration contours. Tunnel outflow velocity is 3 m s^{-1}. Note the plume displacement of 12 m as well as the unfavorable suction of polluted air into the other tunnel.

First, the flow conditions inside a one-directional tunnel were investigated. Vehicle traffic moving with 80 km h^{-1} was substituted in the simulation by momentum sources determined from drag coefficient c_D, vehicle cross-section A_{veh}, and the traffic density. The piston effect of a single vehicle can be expressed according the Swiss standard (*ASTRA*, 2004) by the pressure difference caused by it:

$$0.5\rho(u_{veh}-u_{air})^2 c_D A_{veh} A_{tunnel}^{-1}. \quad (1)$$

In the FLUENT simulation utilizing this assumption, at maximal traffic density and without the use of a longitudinal tunnel ventilation system, an average tunnel air velocity u_{air} of 1.8 m s^{-1} was developed.

Following this simulation, the tunnel portal model was placed in an atmospheric boundary layer flow to observe the pollutant plume's displacement at several wind directions. The simulations utilized the RANS approach with standard k–ε turbulence closure on a mesh consisting of 800,000 tetrahedral and polyhedral cells. External flow velocity was 3 m s^{-1} at 100 m height, tunnel air velocity was also 3 m s^{-1}. Simulation at cross-flow wind showed a plume displacement of about 12 m from the tunnel portal (*Fig. 5*, right). Remarkably, the other one-directional tunnel is sucking in a part of polluted air released by

the other tunnel. (This short-circuit is unfavorable and can be prevented by increasing the distance between the two portals, e.g., shifting the two portals away in longitudinal direction, or by building a separation wall between them.)

Based on the results mentioned, the pollutants sources in the MISKAM simulations were placed 10 m in front of the portals. To account for the high concentration gradients, the grid density in the portal region was increased to 5 m × 7.5 m × 1.5 m.

3.3. Wind tunnel testing

Wind tunnel testing proved to be a sufficient physical modeling method of the real scale dispersion processes in the past (*Cermak*, 1984; *Plate*, 1999), and thus, it can serve as reference data source for the current CFD simulations.

As in most environmental wind tunnels, only the modeling of neutral conditions was possible in the current wind tunnel test campaign. The atmospheric boundary layer profile was modeled by a horizontal grid, spikes, and roughness elements (*Fig. 6*) and was checked by two-component hot-wire measurements (cross-wire sensor with DISA 55M CTA bridges). The profile measurement results are shown in *Fig. 7*.

The wind tunnel measurements were carried out on a modular 1:1000 scale model with a total area of 28.5 m^2 (largest extents about 8 m × 5 m), resolving the topography, buildings, vegetation, and pollutant sources of the surroundings. From the modules, models of the three junctions at various wind directions and route alternatives could be constructed and investigated separately in the wind tunnel. The elevation at the model boundaries was relaxed to zero level using artificial slopes.

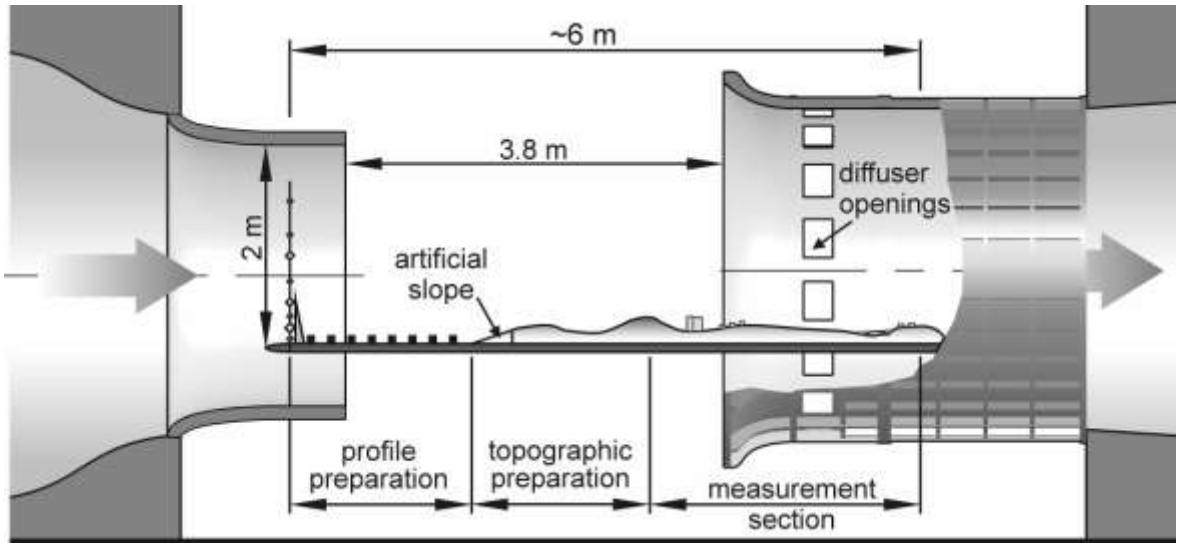

Fig. 6. Vertical cross section view of the model arranged in the test section of the Göttingen-type wind tunnel.

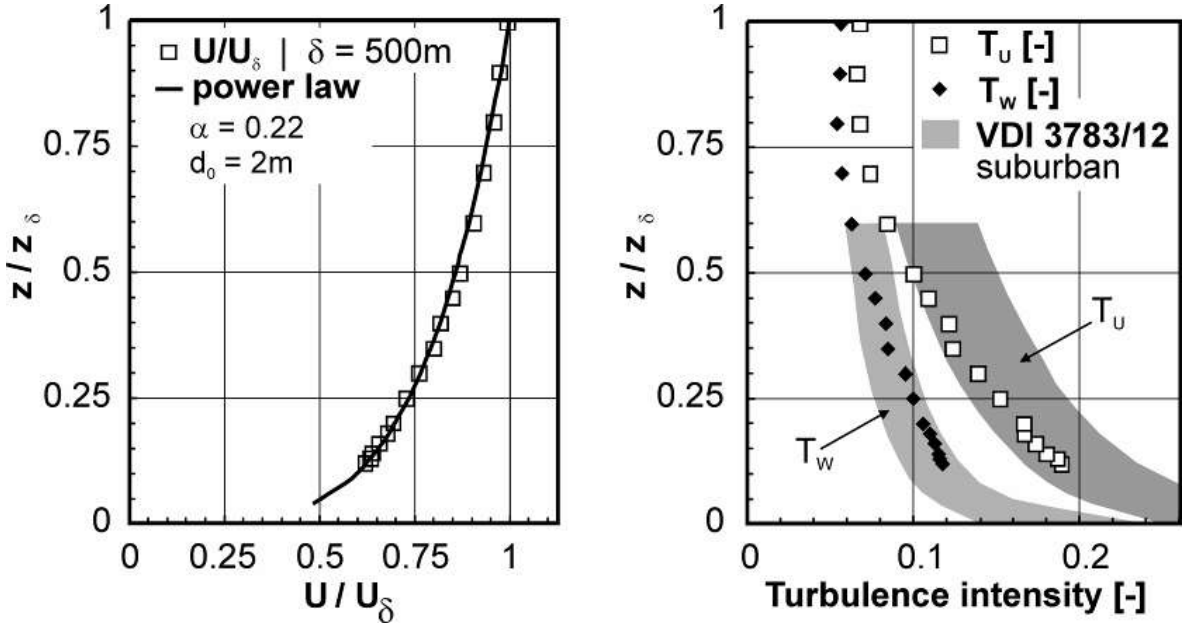

Fig. 7. Inlet profiles of mean velocity and turbulence measured by two-component CTA. The reference height δ is 500 m at full scale.

Fifty sampling points were distributed on the model (see black dots in *Fig. 1*) near tunnel portals and road sections, and inside inhabited areas and locations of specific care, for example at school buildings. Unfortunately, detailed concentration field mapping along lines or arcs could not be fitted into the four-month timeframe of the wind tunnel tests.

Methane was used as tracer gas, and source strengths Q_i were controlled using digital mass flow controllers. Road segments were treated as line sources, and therefore, tracer was released from underfloor source units lying in line with the model's surface. The construction ensured homogeneous exhaust along the road following the line source construction principle of *Meroney et al.* (1996). The pollutants produced in the road tunnels were supposed to leave the tunnel at the portal in the direction of traffic and were modeled accordingly as point sources with a small horizontal momentum. Air samples were collected simultaneously by an automatic 24-channel sampling system built from stepmotor-driven sampling cylinders and magnetic valves, and they were analyzed by a flame ionization detector (FID) afterwards. The system was calibrated with gas samples of known concentration. Repeatability tests of the whole measurement system gave an average relative uncertainty of 9% over a range of 10^2–10^4 ppm CH_4 concentration.

To a further check of the concentration measurement system, a simple test case known from the literature was measured, consisting of a line source placed into a crosswind boundary layer flow. The measured concentration downwind the source was inside the limits given by the VDI guideline 3783/12 (*VDI*, 2004). This test also proved that the use of methane as tracer

gas, regardless of its different density is proper, if testing wind speed is high enough, and thus, buoyancy effects are suppressed.

Afterwards, the Reynolds number dependency of concentration results was checked on the terrain model by repeating concentration measurements at different wind speeds. It was found that above the mean flow velocity u_{ref} of 3 m s^{-1} (at H_{ref} = 50 mm height), normalized concentrations

$$c^+ = c u_{ref} H_{ref}{}^2 Q^{-1} \tag{2}$$

remain constant, thus independent of the Reynolds number. In the final tests, u_{ref} was set to 4.5 m s^{-1}.

The horizontal momentum of polluted air inlet at the tunnel portals was determined by keeping the ratio of tunnel air momentum and incident wind momentum ($\rho_Q u_Q{}^2 \rho_{air}{}^{-1} u_{ref}{}^{-2}$) constant in both full and model scale. This gave 3 m s^{-1} model scale tunnel air velocity for 2.3 m s^{-1} full scale tunnel air velocity.

In total, 126 sets of concentration measurements, each consisting of 10 to 22 sampling points, were performed. The wind tunnel's background concentration and calibration gas were sampled in each set. The influence of each individual source i (road segment, tunnel portal) on the concentration distribution was measured separately at each wind direction to determine the contribution of the different sources to the total concentration.

Full scale concentrations c_{FS} [g m^{-3}] of NO_X, PM_{10}, and CO at a specific wind direction were determined based on the similarity of normalized concentrations c_i^+ in both model and full scale by taking into consideration the real traffic emissions $Q_{i,FS}$ [g s^{-1}] of the individual sources, and finally by adding the background concentrations c_{bg} from *Table 1*, as

$$c_{FS} = c_{hg} + u_{ref\,FS}{}^{-1} H_{ref\,FS}{}^{-2} \sum c_i^+ Q_{iFS}. \tag{3}$$

4. Results and discussion

As the ratio of the emitted pollutant mass flow and the corresponding concentration limit value is far the highest for NO_x (among the pollutants mentioned above), the distribution maps of NO_x will be analyzed further in Section 4. Although the photochemical reactions, which lead to the formation of more dangerous NO_2 and O_3, were not included in this study, annual mean values of NO_x can be correlated to those of NO_2 based on long-term station observations, and thus, a prediction can be given also for annual NO_2 concentrations.

4.1. General observations

The flow field at the three junctions could be analyzed using velocity profiles, streamlines, and contour plots of the CFD results. An example is shown in *Fig. 8*.

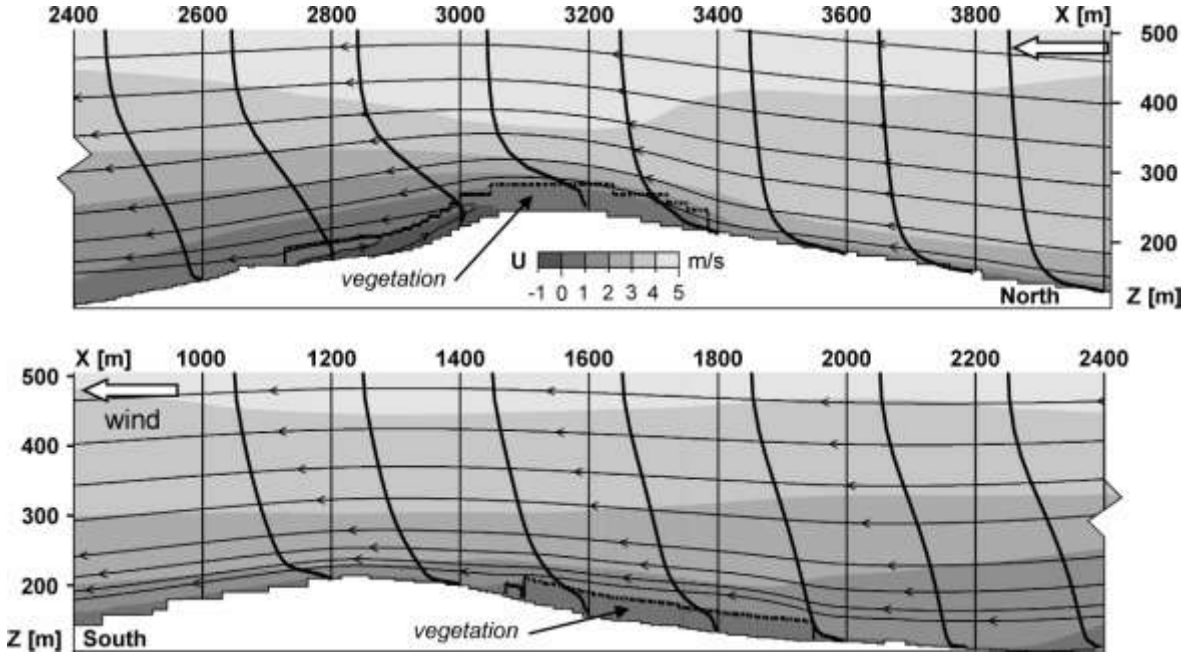

Fig. 8. North-south cross section of the flow over hills of Junction 3 for a north wind with streamlines and vertical profiles of the *U* velocity component. Boundaries of deciduous forests are shown with dotted lines. Note the speedup above the hills and the small separation region and backward flow on the lee side of the northern hill.

The most important factors affecting the flow field are listed in the following:

(1) The influence of topography ranges from slight changes of wind direction and wind speed to the full three-dimensionality of flow. Speed-up could be observed above the hill ridges. Separation zones can develop behind steeper hills (see at Junction 3 in *Fig. 8* and later in *Fig. 12*).

(2) Building effects are only worth mentioning near the 10–15 storey block buildings of Junction 1, while at the other junctions detached houses of suburban towns act rather like roughness elements because the grid resolution is not sufficient to resolve the small flow structures around them (buildings accommodate only a few grid cells).

(3) Vegetation zones are slowing down the flow and at the same time shifting the main flow upwards (*Fig. 8*).

Based on both wind tunnel measurements and CFD simulations we can draw the following conclusions about the concentration field:

(1) In the case of road segments running on the surface, concentration limits are exceeded only in a narrow strip of about 50 m along the road.

(2) On the other hand, the emission from tunnel portals can cause plumes of more than 100 m length above the hourly concentration limit (200 μg m^{-3}), reaching even populated areas (*Fig. 9*).

(3) The direction of the tunnel plumes is slightly modified by the topography; see, for example, at Junction 2 with a northeast wind direction (*Fig. 9*).

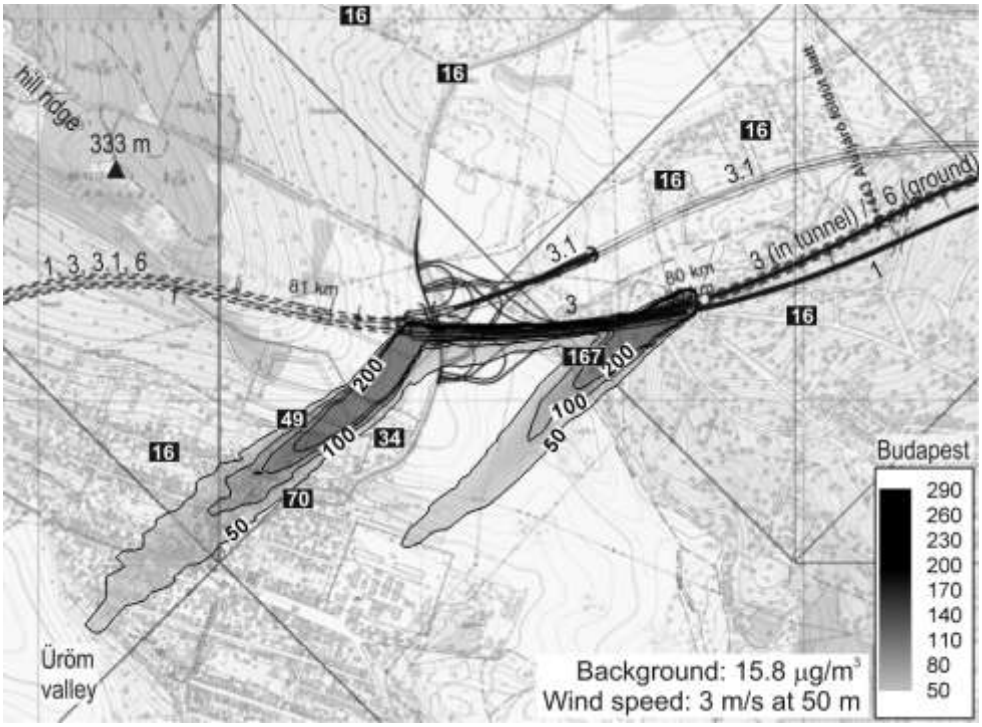

Fig. 9. Concentrations of NO_x [μg m^{-3}] at Junction 2, 3 m above the surface with a NE wind direction and a wind velocity of 3 m s^{-1}, in the case of route alternative 3 without ventilation stacks operating. White numbers: concentrations from wind tunnel measurement, contour plot; bold black numbers: simulation results. (The other route alternatives are drawn in the figure but are not in operation.)

(4) In separation zones, upwind dispersion is possible due to the recirculating flow.

(5) Pollution coming from viaducts has an almost negligible footprint at the surface due to the higher wind speed and the higher altitude of release (*Fig. 12*).

4.2. Modeling of ventilation stacks

To account for the most prominent observation made in Section 4.1, the large pollutant plumes released from tunnel portals, which threaten the air quality of nearby settlements at low wind speeds and rush-hour traffic density, the design of the tunnel ventilation system was extended by ventilation stacks. These will be put into operation if the above mentioned conditions are met and will then exhaust the polluted tunnel air at more than 20 m height above ground. In this way, large concentrations at ground level in the vicinity of the portals can be avoided. In *Fig. 10*, the revised ventilation concept can be seen. The stacks are located near the tunnel portals.

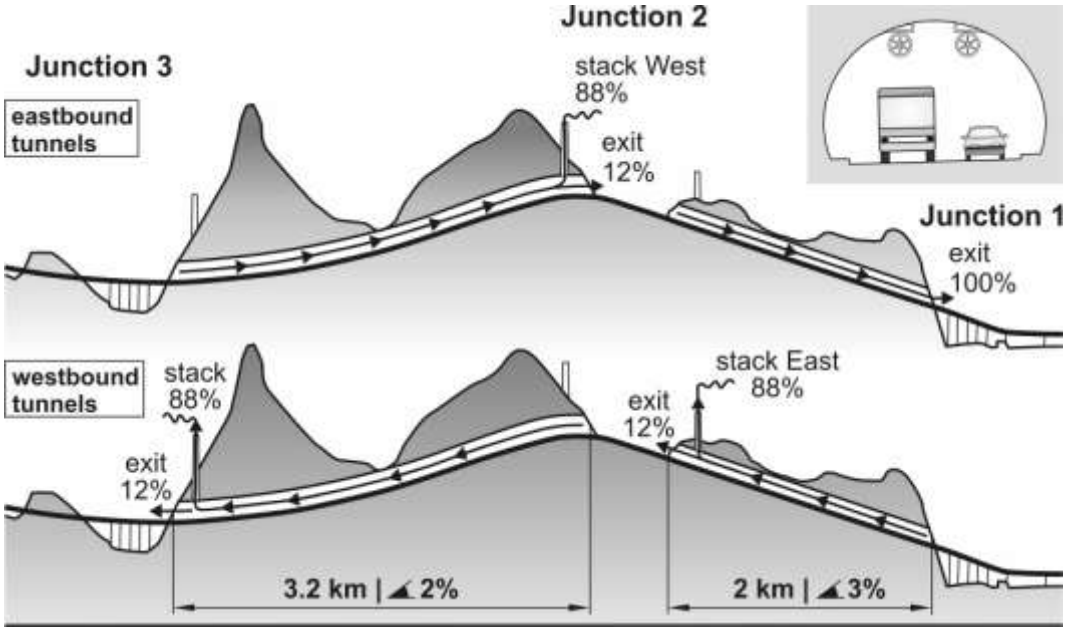

Fig. 10. Tunnel ventilation concept with stack locations. The ventilation of the eastbound and westbound one-directional tunnels is independent, and thus, shown separately. Elevation is scaled approximately by 10. Upper right corner: cross-section of a one-directional tunnel with axial ventilation fans.

The concept was checked in further MISKAM simulations. Stack heights range between 20–25 m, and vertical outflow velocity of the exhaust was set to 6 m s^{-1}. Based on the simulation results, if external wind speed is 3 m s^{-1} at 50 m height, at least 88% of the polluted tunnel air has to be exhausted through the stacks to avoid concentration limit exceedance near the portals. When comparing *Figs. 9* and *11*, the decrease of the area with concentrations above the hourly concentration limit (200 μg m^{-3}) is obvious, while footprints of stack plumes on the surface are well below the limit. The plume of the west stack is also modified by the topography, more specifically by the NW oriented nearby hill ridge.

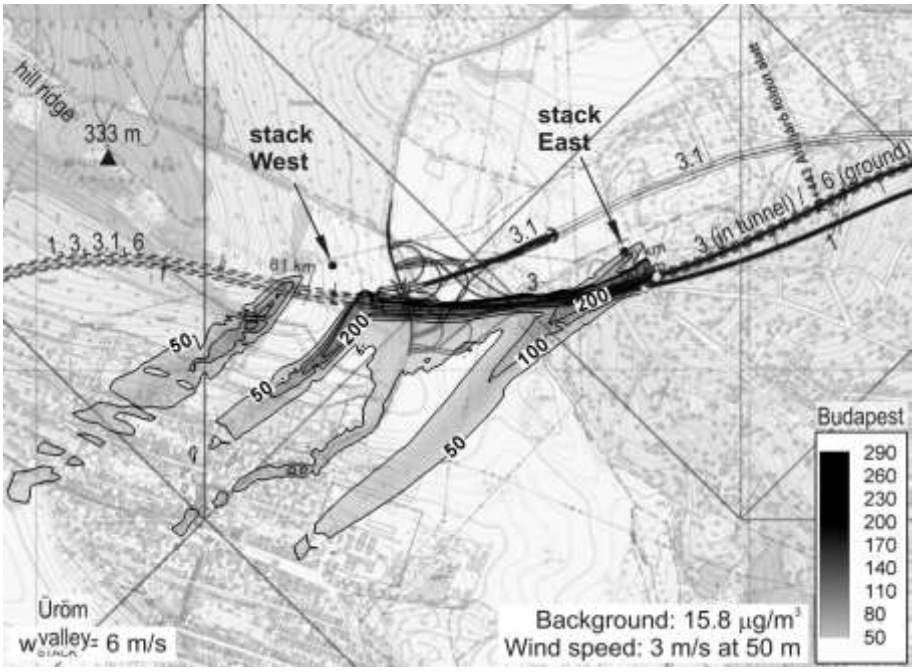

Fig. 11. Concentrations of NO_x [µg m^{-3}] at Junction 2, 3 m above the surface with a NE wind direction and a wind velocity of 3 m s^{-1}, in case of route variant 3. Ventilation stacks are in operation, vertical stack velocity is 6 m s^{-1}. Compare this figure to *Fig. 9*.

Detailed analysis of the flow and concentration fields showed that plume axes run at about 40 m height above ground (see *Fig. 12*). Surface concentrations below the stack plumes are significantly smaller than those at the tunnel portals, although they exhaust seven times more pollutant. *Fig. 12* also demonstrates the ability of CFD models in resolving three-dimensional flows above complex terrain.

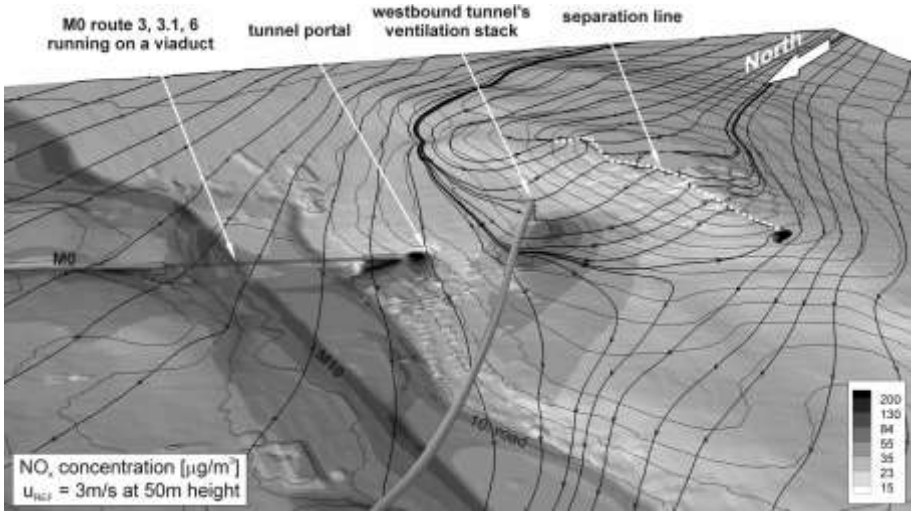

Fig. 12. MISKAM simulation of Junction 3 with a north wind direction and 3 m s^{-1} wind velocity at 50 m height. Tunnel ventilation stacks are in operation. Streamlines (thicker black lines) at 6 m height above ground show a separation behind the northern hill and the modification of the ventilation stack's plume centerline (dark grey rod). Thin black lines: topographic level curves; surface color: concentration (logarithmic scale).

To decrease the power consumption of the ventilation system, it is proposed to operate it only at lower wind speeds with full power. In case of higher wind speeds pollutant dilution is faster, thus, a larger portion of polluted tunnel air can be released through the portal without causing limit exceedances. Similarly, in periods with low traffic, further ventilation energy can be saved.

4.3. Comparison of experimental and numerical results

The comparison of experimental and numerical concentrations (in total 499 non-zero value pairs) in the left part of *Fig. 13*, shows acceptable agreement in general. However, some larger deviations were observed, which are partly due to limitations of the modeling methods. The deviations were analyzed point by point and the most typical causes found are listed in the following.

(1) Known limitations of $k-\varepsilon$ models: *Castro et al.* (2003) concluded from their Askervein Hill simulations that speed-up above the hilltop is underpredicted. Furthermore, being originally a steady-state simulation, the time-dependency, especially in recirculating zones, is not captured by the models. In our case this is not problematic, as we are interested in mean values only. Concerning the dispersion results, according to the validation tests in *Eichhorn* and *Balczó* (2008), MISKAM 5 predicts thinner and longer pollutant plumes from point sources than those measured in wind tunnel.

(2) Minor geometrical differences between the wind tunnel and numerical model: Near the line sources very large concentration gradients can occur, meaning that even a small displacement of a sampling point in the physical and numerical model could cause errors of above 50%.

(3) Different initial dilutions of the pollutant sources can again affect near-source measurements (passive scalar released in source grid cells in CFD vs. tracer gas released along a line from the surface of the wind tunnel model).

(4) Different vegetation modeling: In the numerical model, the parameter expressing the vegetation density, known as leaf area density (*LAD*), was 0.5, an average value for deciduous forests taken from the literature. This corresponds according to *Balczó et al.* (2009) and *Gromke* and *Ruck* (2009) at the model scale of 1:1000 to a crown porosity of about 96–97% in the wind tunnel measurement. In the physical model, however, artificial grass of lower porosity was used for forest modeling (approximately 94%), leading to smaller wind velocities and higher displacement thicknesses in vegetation covered areas.

(5) Coarse numerical grid resolution: Because of the staggered grid (without terrain-following coordinate system), slopes, especially in the

inflow and outflow zones, have higher roughness, influencing the near-surface balance of *k* and, in consequence, the dispersion.

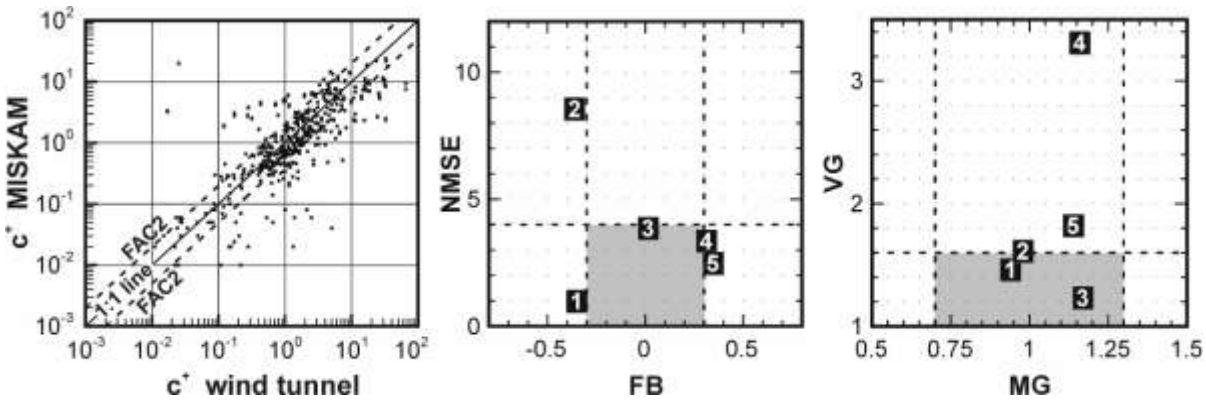

Fig. 13. Left: logarithmic scatter plot of measured and simulated concentrations c^+. The plot contains all non-zero value pairs which were measured respectively simulated in the 50 sampling point locations (see *Fig. 1*), in total about 499 points. Dashed lines show 50% and 200% of the measurements. Points between the two lines represent predictions within a factor of two of observations (FAC2).

Middle and right: Plots of linear and logarithmic validation metrics of normalized concentration c^+ from different MISKAM simulations. Cases compared: (1) perpendicular flow in a street canyon with vegetation of *Balczó et al*. (2009); (2) simulation of the Mock Urban Setting Test (*Eichhorn* and *Balczó*, 2008) using MISKAM 5.02; (3) simulation of the Mock Urban Setting Test using MISKAM 6; (4) present simulation, all non-zero values; and (5) present simulation, all values > 0.5. The model acceptance range is marked grey.

4.4. Validation metrics

To quantify the extent of deviations between results from numerical and physical modeling, statistic metrics after *Chang* and *Hanna* (2004) were calculated. The values can be seen in *Table 5*; many of them are within or at least close to the limits of acceptance proposed for state-of-the-art models. The larger positive value of the fractional bias (FB) shows that wind tunnel results are moderately underestimated by the simulation at large concentrations. However, this is not the case at medium and small concentrations, because geometric mean bias (MG), which is not dominated by the large concentration values, is very good. The worse value of geometric variance (VG) while at the same time the normal mean square error (NMSE) is clearly inside the limit, can be explained by the scattering of small concentration values due to the measurement error. After filtering c^+ values smaller than 0.5, metrics of the remaining 336 data points improve significantly.

In *Fig.13*, middle and right, one can see the metrics of concentrations from already published validation studies using the MISKAM code. Point 1 of the figure refers to a simulation in a street canyon with a building height to street width ratio of 1:1 and a street length to width ratio of 10:1, at perpendicular flow direction and with tree planting inside the canyon, described in detail in *Balczó et al*. (2009).

Table 5. Calculated statistic metrics for concentration (after *Chang* and *Hanna*, 2004)

Validation metric	**Abbre-viation**	**Limit**	**All non-zero values**	**Values < 0.5 filtered**	**Classification**
Correlation coefficient	R	0.8	0.608	0.722	Fair
Fractional bias	FB	± 0.3	0.313	0.347	Nearly good
Normalized mean square error	NMSE	$0-4$	3.35	2.47	Good
Geometric mean bias	MG	0.7–1.3	1.16	1.14	Good
Geometric variance	VG	0–1.6	3.31	1.82	Nearly good
Fraction of predictions within a factor of two of observations	FAC2	0.5	0.655	0.723	Good

Points 2 and 3 show test results from the Mock Urban Setting Test (*Eichhorn* and *Balczó*, 2008). The Mock Urban Setting Test (MUST) was a full-scale measurement campaign on a rectangular grid-like arrangement of 120 standard shipping containers in Utah as described by *Yee* and *Biltoft* (2004), wind tunnel tests of the same arrangement were carried out by *Leitl et al*., (2007). MISKAM was used to simulate dispersion from a source between the containers at slanted $-45°$ flow. Tracer dispersion data was compared in 256 data points. This test case was run with the current and future MISKAM versions 5.02 (point 2 in *Fig. 13*) and 6 (point 3).

Point 4 refers to all non-zero c^+ values of the current study, point 5 to all c^+ values larger than 0.5. A comparison of these data with those mentioned above indicates clearly, that in case of practical applications and complex geometries like this investigation, the code performs less accurately, but an acceptable level of accuracy can be still achieved.

5. Conclusions

The current paper gives an overview about a larger microscale CFD and wind tunnel test campaign performed in a suburban area of complex terrain in the north of Budapest. Emission determination, mesoscale influences on local wind statistics, and background concentrations were also discussed.

The CFD simulations and accompanying wind tunnel measurements showed that open road sections cause limit exceedance along a narrow strip of some 50 m along the investigated motorway routes, while pollutant plumes from the tunnel portals can spread more hundred meters away. They also provided information on the necessary changes of the tunnel ventilation system. The effect of the proposed ventilation stacks on air quality was estimated by CFD. The NO_x concentration maps delivered by this investigation helped the authorities to select the final route, which is a slightly modified version of route alternative 3.1.

Numerical simulation using the RANS approach with $k-\varepsilon$ closure proved to be a reliable tool to understand and predict flow and dispersion phenomena, resolving all main features of the three-dimensional flow, but deviations from the

experimental results signal that the use of wind tunnel or on-site reference data is still useful. These can provide valuable information for the evaluation and assessment of simulation results, as shown here with the application of statistic metrics.

***Acknowledgements*—**Thanks are due to the Hungarian Meteorological Service, to department staff members *Tamás Régert*, *Viktor Szente*, *Zoltán Szucsán*, *Gábor Kalmár*, and finally to all participating students for their valuable contributions. The investigations presented in this paper were financed by the National Infrastructure Development Corporation of Hungary. This work is connected to the scientific program of the "Development of quality-oriented and harmonized R+D+I strategy and functional model at BME" project, which is supported by the New Széchenyi Plan (grant agreement no.: TÁMOP-4.2.1/B-09/1/KMR-2010-0002). *Miklós Balogh's* participation was also financed by his current project, which is supported by the European Union and co-financed by the European Social Fund (grant agreement no. TÁMOP 4.2.1./B-09/1/KMR-2010-0003).

References

ASTRA, 2004: *Guideline for the ventilation of road tunnels.* ASTRA Bundesamt für Strassen/Swiss Federal Roads Office FEDRO, Bern.

Ayotte, K., Hughes, D., 2004: Observations of boundary-layer wind-tunnel flow over isolated ridges of varying steepness and roughness. *Bound.-Lay. Meteorol. 112*, 525-556.

Balczó, M., Gromke, C., Ruck, B., 2009: Numerical modeling of flow and pollutant dispersion in street canyons with tree planting. *Meteorol Z. 18*, 197-206.

Belcher, S.E., Hunt, J.C.R., 1998: Turbulent flow over hills and waves. *Annu. Rev. Fluid. Mech. 30,* 507-538.

Berkowicz, R., 2000: A simple model for urban background pollution. *Environ. Monit. Assess. 65,* 259-267.

Bettelini, M., Brandt, R., Riess, I., 2001: Environmental aspects of tunnel ventilation. *AITES-ITA 2001 World Tunnel Congress*, Milano, June 10-13, 2001.

Bowen, A. J., 2003: Modelling of strong wind flows over complex terrain at small geometric scales. *J Wind. Eng. Ind. Aerod. 91,* 1859-1871.

Brodeur, P., Masson, C., 2006: Numerical simulations of wind distributions over very complex terrain. *44th AIAA Aerospace Sciences Meeting and Exhibit*, 9–12 January 2006, Reno, Nevada AIAA 2006-1362.

Castro, F.A., Palma, J. M. L. M., Silva Lopes, A., 2003: Simulation of the Askervein flow. Part 1: Reynolds averaged Navier-Stokes equations (k−ε turbulence model). *Bound.-Lay. Meteorol 107,* 501-530.

Cermak, J. E. 1984: Physical modelling of flow and dispersion over complex terrain. *Bound.-Lay. Meteorol. 30,* 261-292.

Chang, J.C., Hanna, S. R., 2004: Air quality model performance evaluation. *Meteorol. Atmos. Phys. 87,* 167-196.

Colberg, C. A., Tona, B., Stahel, W. A., Meier, M., Staehelin, J., 2005: Comparison of a road traffic emission model (HBEFA) with emissions derived from measurements in the Gubrist road tunnel, Switzerland. *Atmos. Environ. 39,* 4703-4714.

Contini, D., Procino, L., Massini, M., Manfrida, G., 2003: Ground-level diffusion of pollutant emitted at the portal of a road tunnel model. *Proceedings of PHYSMOD 2003 International Workshop on Physical Modelling of Flow and Dispersion Phenomena*, Prato, Italy, 244-251.

Cremades, L., 2000: Estimating the background air concentration excluding the contribution of an individual source. *Environ. Model. Assess. 5,* 119-124.

Dixon, N., Tomlin, A., 2007: A Lagrangian stochastic model for predicting concentration fluctuations in urban areas. *Atmos. Environ. 41,* 8114-8127.

Donnelly, R., Lyons, T., Flassak, T., 2009: Evaluation of results of a numerical simulation of dispersion in an idealised urban area for emergency response modelling. *Atmos. Environ. 43,* 4416-4423.

Eichhorn, J., 2008: MISKAM Manual for version 5. giese-eichhorn environmental meteorological software, Wackernheim, Germany

Eichhorn, J., Balczó, M., 2008: Flow and dispersal simulations of the Mock Urban Setting Test. The 12th Int. Conf. on Harmonization within Atmospheric Dispersion Modelling for Regulatory Purposes (HARMO12), Cavtat, Croatia, October 6-9, 2008. *Croatian Meteorol. J. 43*, 67-72.

Eichhorn, J., Kniffka, A., 2010: The numerical flow model MISKAM: State of development and evaluation of the basic version. *Meteorol. Z. 19*, 81-90.

Franke, J., Hellsten, A., Schlünzen, H., Carissimo, B., 2007: *Best practice guideline for the CFD simulation of flows in the urban environment*. COST Office Brussels ISBN: 3-00-018312-4.

Goricsán, I., Balczó, M., Régert, T., Suda, J. M., 2004: Comparison of wind tunnel measurement and numerical simulation of dispersion of pollutants in urban environment. *International Conference on UrbanWind Engineering and Building Aerodynamics, von Karman Institute*, Rhode-Saint-Genése, Belgium, May 5-7, 2004 D.6.1-D.6.10.

Goricsán, I., Balczó, M., Czáder, K., Rákai, A., Tonkó, C., 2011: Simulation of flow in an idealised city using various CFD codes. *Int. J. Environ. Pollut. 44*, 359-367.

Gromke, C., Ruck, B., 2009: On the impact of trees on dispersion processes of traffic emissions in street canyons. *Bound.-Lay. Meteorol. 131*, 19-34.

Holmes, N., Morawska, L., 2006: A review of dispersion modelling and its application to the dispersion of particles: An overview of different dispersion models available. *Atmos. Environ. 40*, 5902-5928.

Infras, 2004: *The Handbook of Emission Factors for Road Transport (HBEFA 2.1).*www.hbefa.net, CD-ROM database.

Jones, A. M., Yin, J., Harrison, R. M. 2008: The weekday-weekend difference and the estimation of the non-vehicle contributions to the urban increment of airborne particulate matter. *Atmos. Environ. 42*, 4467-4479.

Kaimal, J., Finnigan, J., 1994: *Atmospheric Boundary Layer Flows.* Oxford University Press.

Kato, M., Launder, B., 1993: The modelling of turbulent flow around stationary and vibrating square cylinders. *Ninth Symp. on Turbulent Shear Flows*, Kyoto, Japan, August 1993, 10.4.1-10.4.6.

Ketzel, M., Berkowicz, R., Lohmeyer, A., 2000: Comparison of numerical street dispersion models with results from wind tunnel and field measurements. *Environ. Monit. Assess. 65*, 363-370.

Ketzel, M., Louka, P., Sahm, P., Guilloteau, E., Sini, J. F., Moussiopoulos, N., 2002: Intercomparison of numerical urban dispersion models - Part II: Street canyon in Hannover, Germany. *Water Air Soil Pollution: Focus 2*, 603-613.

Ketzel, M., Omstedt, G., Johansson, C., Düring, I., Pohjola, M., Oettl, D., Gidhagen, L., Wahlin, P., Lohmeyer, A., Haakana, M., Berkowicz, R., 2007: Estimation and validation of PM2.5/PM10 exhaust and non-exhaust emission factors for practical street pollution modelling. *Atmos. Environ. 41*, 9370-9385.

Kim, H. G., Patel, V. C., 2000: Test of turbulence models for wind flow over terrain with separation and recirculation. *Bound.-Lay. Meteorol. 94*, 5-21.

Kristóf, G., Rácz, N., Balogh, M., 2009: Adaptation of pressure based CFD solvers for mesoscale atmospheric problems. *Bound.-Lay. Meteorol. 131*, 85-103.

Leitl, B., Bezpalcova, K., Harms, F., 2007: Wind tunnel modelling of the MUST experiment. *The 11th International Conference on Harmonisation within Atmospheric Dispersion Modelling for Regulatory Purposes (HARMO11)*. Cambridge, UK, July 2–5. 435-439.

Liu, H., Zhang, B., Sang, J., Cheng, A. Y. S., 2001: A laboratory simulation of plume dispersion in stratified atmospheres over complex terrain. *J. Wind Eng. Ind. Aerod. 89*, 1-15.

Lohmeyer, A., Mueller, W. J., Baechlin, W., 2002: A comparison of street canyon concentration predictions by different modellers: final results now available from the Podbi-exercise. *Atmos. Environ. 36*, 157-158.

Longley, I., Kelly, F., 2008: Systematic literature review to address air quality in and around traffic tunnels. *National Health and Medical Research Council*, Commonwealth of Australia.

López, S. D., 2002*:* Numerische Modellierung turbulenter Umströmungen von Gebäuden. *PhD thesis, University of Bremen*, Germany.

McBride, M., Reeves, A., Vanderheyden, M., Lea, C., Zhou, X., 2001: Use of advanced techniques to model the dispersion of chlorine in complex terrain. *Process. Sa. Environ. 79*, 89-102.

Mensink, C., De Ridder, K., Deutsch, F., Lefebre, F., Van de Vel, K., 2008: Examples of scale interactions in local, urban, and regional air quality modelling. *Atmos. Res. 89*, 351-357.

Meroney, R.N., Pavageau, M., Rafailidis, S., Schatzmann, M., 1996: Study of line source characteristics for 2-D physical modelling of pollutant dispersion in street canyons. *J. Wind Eng. Ind. Aerod. 62,* 37-56.

Moussiopoulos, N., Flassak, T., Knittel, G., 1988: A refined diagnostic wind model. *Environ. Softw. 3,* 85-94.

Nadel, C., Vanderheyden, M. D., Lepage, M., Davies, A., Wan, P., Ginzburg, H., Schattanek, G., 1994: Physical modelling of dispersion of a tunnel portal exhaust plume. *8th International Symposium on Aerodynamics & Ventilation of Vehicle Tunnels*, Liverpool, UK.

Oettl, D., Sturm, P., Almbauer, R., Okamoto, S., Horiuchi, K., 2003: Dispersion from road tunnel portals: comparison of two different modelling approaches. *Atmos. Environ. 37,* 5165-5175.

Olesen, H., Berkowicz, R., Ketzel, M., Løfstrøm, P., 2009: Validation of OML, AERMOD/PRIME and MISKAM using the Thompson wind-tunnel dataset for simple stack-building configurations. *Bound.-Lay. Meteorol. 131,* 73-83.

Palma, J., Castro, F., Ribeiro, L., Rodrigues, A., Pinto, A., 2008: Linear and nonlinear models in wind resource assessment and wind turbine micro-siting in complex terrain. *J. Wind. Eng. Ind. Aerod. 96,* 2308-2326.

Plate, E.J. (ed.), 1982: *Engineering Meteorology.* Elsevier.

Plate, E. J., 1999: Methods of investigating urban wind fields – physical models. *Atmos. Environ. 33,* 3981-3989.

Ries, K., Eichhorn, J., 2001: Simulation of effects of vegetation on the dispersion of pollutants in street canyons. *Meteorol. Z. 10,* 229-233.

Rodrigues, C. A. V., 2005: Analysis of the atmospheric boundary layer flow over mountainous terrain. *Master's thesis, Von Karman Institute.*

Sahm, P., Louka, P., Ketzel, M., Guilloteau, E., Sini, J. F., 2002: Intercomparison of numerical urban dispersion models – Part I: Street canyon and single building configurations. *Water Air Soil Poll: Focus 2,* 587-601.

Silva Lopes, A., Palma, J., Castro, F., 2007: Simulation of the Askervein flow. Part 2: Large-eddy simulations. *Bound.-Lay. Meteorol. 125,* 85-108.

Smolarkiewicz, P., Grabowski, W., 1989: The multidimensional positive definite advection transport algorithm: Nonoscillatory option. *J. Computat. Phys. 86,* 355–375.

Snyder, W. H., 1990: Fluid modeling applied to atmospheric diffusion in complex terrain. *Atmos. Environ. Part A General Topics. 24,* 2071-2088.

Stern, R., Yamartino, R. J., 2001: Development and first evaluation of Micro-Calgrid: a 3-D, urban-canopy-scale photochemical model. *Atmos. Environ. 35,* 149-165.

Taylor, P. A., Teunissen, H. W., 1987: The Askervein Hill project: Overview and background data. *Bound.-Lay. Meteorol. 39,* 15-39.

Tchepel, O., Borrego, C., 2010: Frequency analysis of air quality time series for traffic related pollutants. *J. Environ. Monitor. 12,* 544-550.

Tchepel, O., Costa, A., Martins, H., Ferreira, J., Monteiro, A., Miranda, A., Borrego, C., 2010: Determination of background concentrations for air quality models using spectral analysis and filtering of monitoring data. *Atmos. Environ. 44,* 106-114.

Vardoulakis, S., Fisher, B. E. A., Pericleous, K., Gonzalez-Flesca, N., 2003: Modelling air quality in street canyons: a review. *Atmos. Environ. 37,* 155-182.

VDI, 2004: VDI 3783, Part 12: Environmental meteorology, Physical modelling of flow and dispersion processes in the atmospheric boundary layer. *Application of Wind Tunnels.* Beuth-Verlag, Germany.

VDI, 2005: *VDI 3783, Part 9:* Environmental meteorology. Prognostic microscale windfield models: *Evaluation for Flow Around Buildings and Obstacles.* Beuth-Verlag, Berlin, Germany.

Walmsley, J. L., Taylor, P. A., 1996: Boundary-layer flow over topography: Impacts of the Askervein study. *Bound.-Lay. Meteorol. 78,* 291-320.

Wood, N., 2000: Wind flow over complex terrain: A historical perspective and the prospect for large-eddy modelling. *Bound.-Lay. Meteorol. 96,* 11-32.

Xie, Z. T., Castro, I. P., 2009: Large-eddy simulation for flow and dispersion in urban streets. *Atmos. Environ. 43,* 2174-2185.

Yee, E., Biltoft, C.A., 2004: Concentration fluctuation measurements in a plume dispersing through a regular array of obstacles. *Bound.-Lay. Meteorol. 111,* 363-415.